Role of Arctic Atmospheric Rivers in Driving Wintertime High Arctic Warm Extremes and Their Trends in Recent Decades

Weiming Ma[1], Hailong Wang[1], Gang Chen[2]

[1]Pacific Northwest National Laboratory, Richland, WA, USA; [2]University of California Los Angeles, Los Angeles, CA, USA

1. Motivation

- The Arctic has been warming at a rate 3-4 times faster than the rest of the globe, resulting in a rapid moistening of the local atmosphere.
- Atmospheric rivers (ARs) can effectively drive wintertime warm extremes over the Arctic. Given the rapid warming/moistening of the Arctic, our knowledge on the role of ARs in driving wintertime warm extremes over the high Arctic is limited. Furthermore, there is a lack of comprehensive understanding regarding the trends of Arctic ARs and the associated driving mechanisms.

2. Data and Methodology

- **Data**
  - ➢ Daily and hourly data from ERA5
  - ➢ Daily data from the 50-member CESM2 Large Ensemble (LENS2) with smoothed biomass burning and the 10-member CESM2 Atmosphere-only ensemble (GOGA)
    - ➢ Historical forcing from 1980 to 2014
    - ➢ SSP370 forcing from 2015 to 2021
  - ➢ Daily data from 23 CMIP coupled models
  - ➢ **Warm extremes** occur when the hourly 2-meter air temperature (T2m) over a grid point >= 0℃ over the high Arctic (>= 80°N) during DJF.
- **AR Detection Algorithm**
  - ➢ The integrated water vapor (IVT) based AR detection algorithm of Guan and Waliser (2019) is employed.

3. Concurrent Warming Events

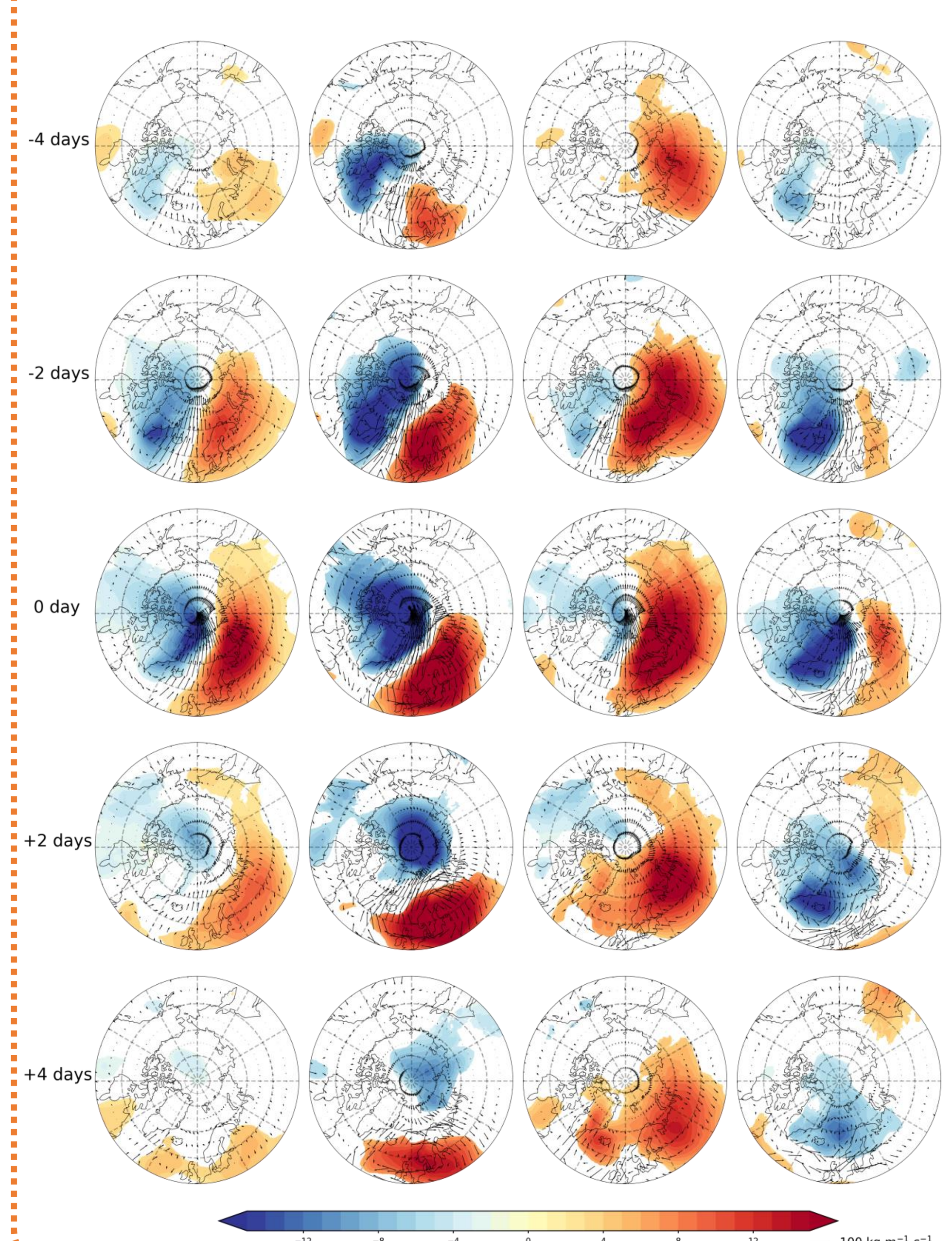

Figure 1. Temporal evolution of the large-scale circulation associated with the concurrent warming events. The shaded contours show the SLP anomalies, and the vectors represent the IVT anomalies. The 1st column describes the composites for all the concurrent warming events. The 2nd, 3rd, and 4th columns show the composites for the 1st, 2nd, and 3rd cluster, respectively, obtained from K-means clustering. Day 0 indicates the time with the largest area where temperature exceeds 0℃.

- ➢ Concurrent warming events are driven by a dipole pattern in the SLP anomalies.
- ➢ k-means clustering applied to the spatiotemporal evolution of these concurrent warming events further reveals that they mainly consist of three different types of SLP spatial patterns: dipole dominance type, anticyclone dominance type, and the cyclone dominance type.

4. Role of ARs

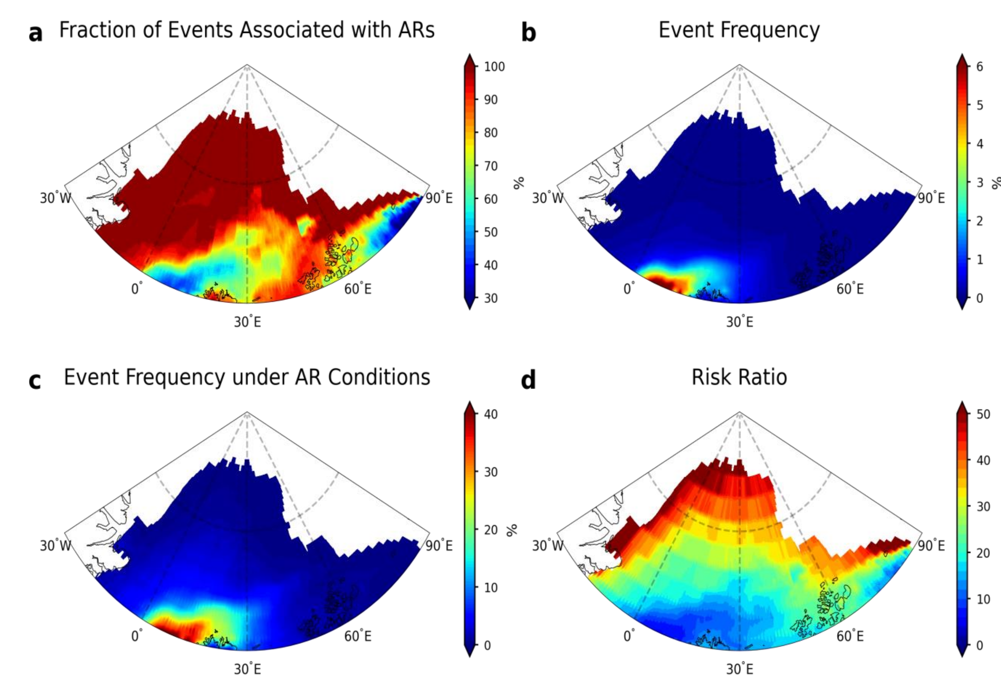

Figure 2. Spatial distribution of (a) the fraction of extreme warming events defined as a grid point with T2m >= 0 °C that occurs during AR days, (b) the fraction of time for all winter hourly snapshots from 1979-2021 with T2m above 0℃, (c) the fraction of time for all AR day hourly snapshots from 1979-2021 with T2m above 0℃, and (d) the risk ratio, which is calculated by dividing (c) by (b).

- ➢ Poleward of about 83°N, 100% of these events occur under AR conditions.
- ➢ ARs increase the risk of extreme warming events dramatically, ranging from about 10 times more likely over lower latitude regions to about 50 times more likely over higher latitude regions.

5. Arctic AR Trends

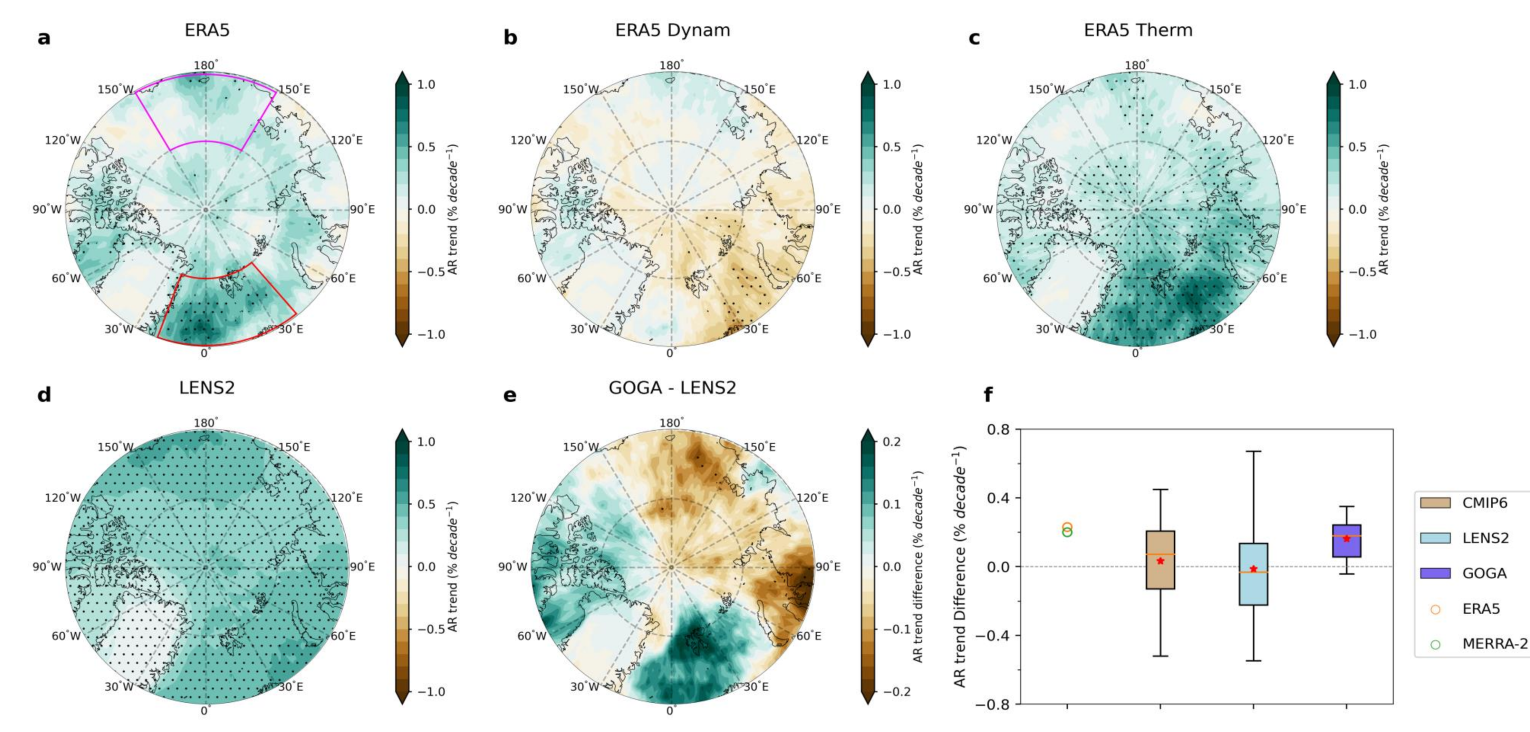

Figure 3. a, Arctic AR frequency trend during 1981–2021 in ERA5. The decomposed dynamical and thermodynamical contributions are shown in **b** and **c**, respectively. **d**, Ensemble mean Arctic AR trend simulated in LENS2. **e**, Difference between the ensemble mean AR trends in GOGA and LENS2 (GOGA – LENS2). **f**, Trend differences between the Atlantic sector and Pacific sector in reanalyses and simulations.

- ➢ In the past four decades, the observed Arctic AR frequency increased by twice as much over the Atlantic sector compared to the Pacific sector due to the faster moistening over the Atlantic sector.
- ➢ Models driven by anthropogenic forcing simulate spatially more uniform Arctic AR trends.
- ➢ Models prescribed with observed SST/sea ice reproduce the stronger Arctic AR trend over the Atlantic sector compared to the Pacific sector.

6. Maximum Covariance Analysis

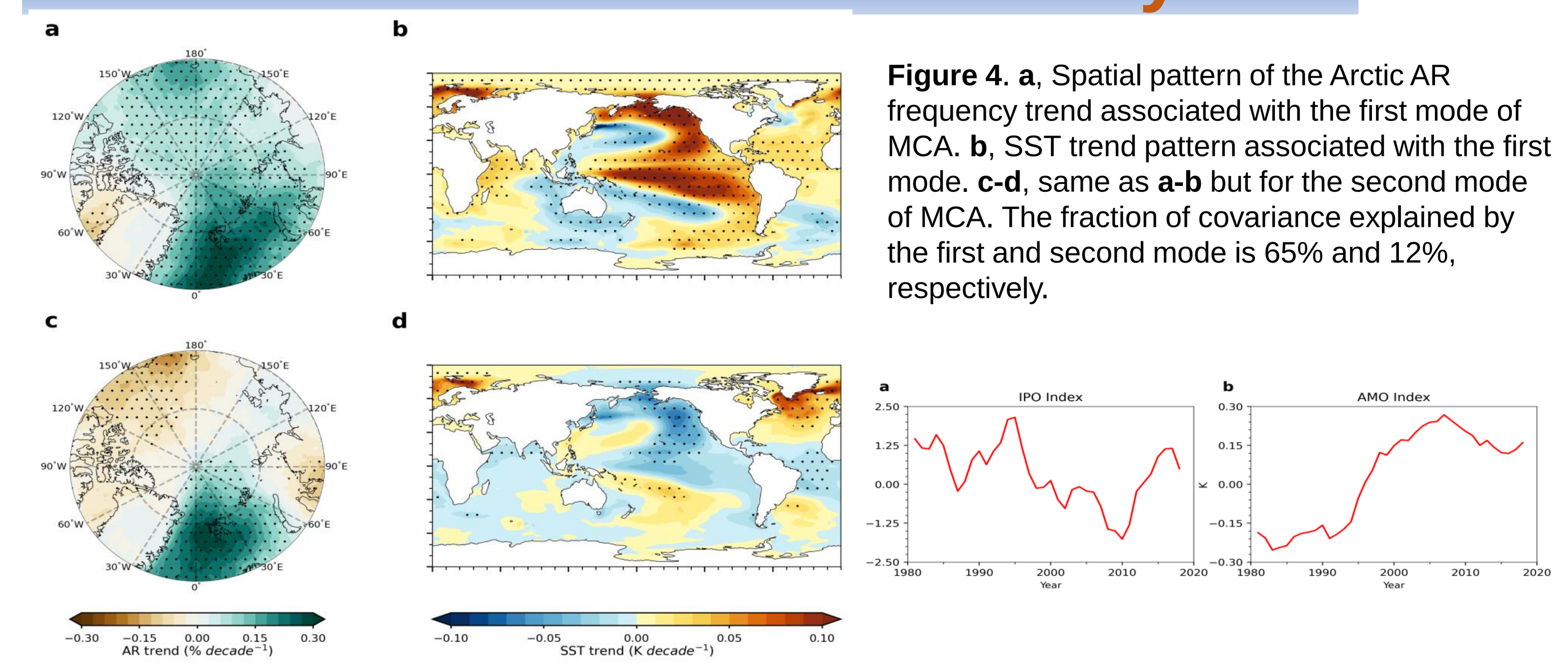

Figure 4. a, Spatial pattern of the Arctic AR frequency trend associated with the first mode of MCA. **b**, SST trend pattern associated with the first mode. **c-d**, same as **a-b** but for the second mode of MCA. The fraction of covariance explained by the first and second mode is 65% and 12%, respectively.

- ➢ The second mode displays a dipole pattern with an increase (decrease) in AR frequency over the Atlantic (Pacific) sector. The corresponding SST trend pattern shows a positive Atlantic Multidecadal Oscillation (AMO) over the North Atlantic and a negative Interdecadal Pacific Oscillation (IPO)-like pattern over the Pacific.
- ➢ In the past four decades, the observed IPO showed an overall negative phase shift, while the AMO exhibited a positive phase shift.

7. Driving Mechanisms

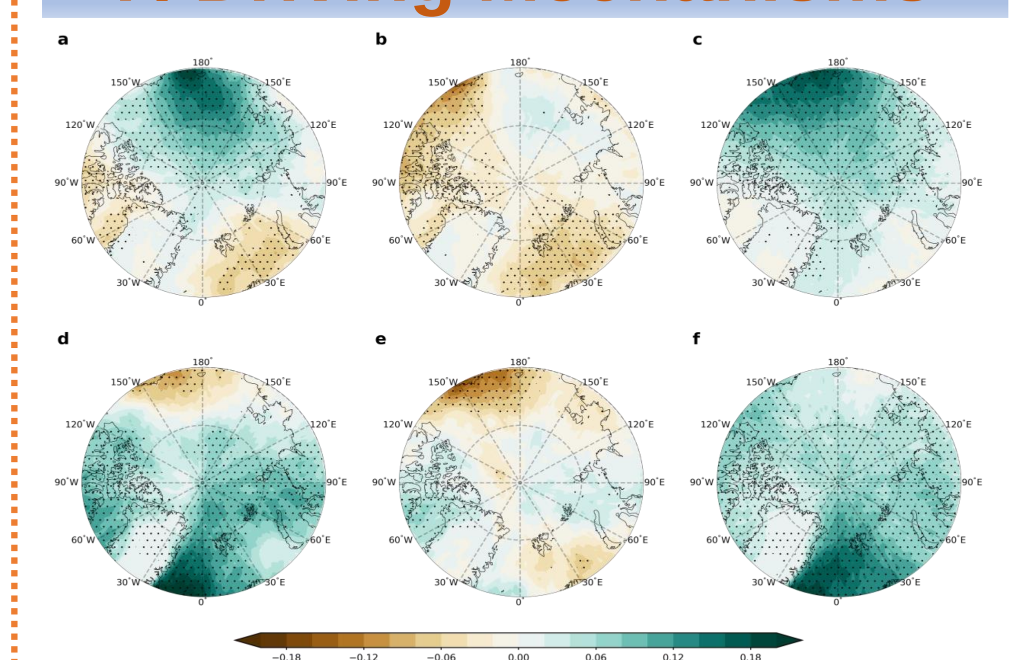

Figure 5. a, Regression pattern of Arctic AR frequency time series onto the standardized IPO index, which represents the total effect of IPO on AR frequency trend. **b**, similar to **a**, but obtained by regressing the Arctic AR frequency time series associated with circulation variability onto the standardized IPO index, which represents the dynamical contribution of IPO to the total AR frequency trend. **c**, obtained by taking the difference between **a** and **b**, representing the thermodynamical contribution of the IPO to the total AR frequency trend. **d-f**, same as **a-c**, but for the AMO.

- ➢ Positive IPO (AMO) increases AR frequency over the Pacific (Atlantic) sector, while reduces it over the Atlantic (Pacific) sector.
- ➢ The present-day combination of negative IPO and positive AMO phase shift favors AR increases (reduction) over the Atlantic (Pacific) sector.

8. Conclusions

- ➢Blocking is a key ingredient in driving wintertime warm extremes.
- ➢Poleward of about 83°N,100% of these events occur under AR conditions..
- ➢In the past four decades, Arctic ARs have been increasing faster over the Atlantic sector compared to the Pacific sector.
- ➢Based on climate models, anthropogenic forcing results in spatially more uniform AR increases over the Arctic.
- ➢The differences between the observed Arctic AR trends and the simulated trends can be reconciled by the observed phase shift of the IPO and AMO.

9. Acknowledgements

This research was supported by the U.S. Department of Energy (DOE), Office of Science, Office of Biological and Environmental Research, Regional and Global Model Analysis program area. This research used resources of the National Energy Research Scientific Computing Center (NERSC), a U.S. DOE Office of Science User Facility operated under Contract No. DE-AC02-05CH11231. The Pacific Northwest National Laboratory (PNNL) is operated for DOE by Battelle Memorial Institute under contract DE-AC05-76RLO1830. W.M acknowledges the travel support provided by US CLIVAR for participation in this workshop.

10. References

1. Weiming Ma, Hailong Wang, Gang Chen, L. Leung et al. The Role of Interdecadal Climate Oscillations in Driving Arctic Atmospheric River Trends. **Under Review**
2. Weiming Ma, Hailong Wang, Gang Chen, Y. Qian et al. Wintertime Extreme Warming Events in the High Arctic: Characteristics, Drivers, Trends, and the Role of Atmospheric Rivers. **Under Review**

PNNL is operated by Battelle for the U.S. Department of Energy

For additional information, contact:
Weiming Ma | weiming.ma@pnnl.gov